Nuclear Physics B251 [FS13] (1985) 254-278

ONE-LOOP PERTURBATIVE CALCULATION OF WILSON LOOPS ON FINITE LATTICES

U. HELLER and F. KARSCH

CERN, Geneva, Switzerland

Received 4 July 1984

We present the one-loop (order g^4) perturbative calculation of the expectation values of Wilson loops and Polyakov lines on finite asymmetric lattices. Analytical as well as numerical results are given. We also give some applications of these results pertaining to the "ratio method", the Coulomb potential on finite lattices, the internal energy of the gluon gas at high temperature and the order parameter of the finite temperature deconfinement transition.

1. Introduction

The formulation of gauge theories on a lattice by Wilson [1], providing a non-perturbative regulator, has opened the way to the application of non-perturbative methods to these theories, most notably Monte Carlo simulations (for reviews, see e.g. [2]). But such simulations are restricted to lattices of rather small size. Non-perturbative measurements require that the correlations length be (much) smaller than the lattice size, which makes it necessary to work at rather large (bare) couplings. The continuum limit, on the other hand, is obtained when the coupling becomes small. To make the results of MC simulations predictive for continuum physics, a connection between MC simulations and perturbation theory has to be established. But when the correlation length becomes large, one has to expect the influence of lattice artifacts to be rather sizeable. Then it becomes important to have control over these lattice effects by doing the perturbation theory on the same finite lattices that are used in MC simulations.

We present here a one-loop calculation (including terms up to order g^4) for the expectation value of Wilson loops and Polyakov lines on lattices of size $V = L^{d-1} \times L_d$ for gauge groups SU(N). Wilson loops have been calculated to order g^4 on a lattice in the temporal gauge by Müller and Rühl [3] for the gauge group SU(2). Due to the particularities of this special choice of gauge, the extraction of values on finite lattices, however, seems to be very cumbersome. For general N, Wilson loops have been computed by several groups using certain continuum approximations [4, 5]. But since it is just the lattice effects that we are interested in, we consider such approximations insufficient for our purpose. While we were involved in the numerical part of our computation, we became aware of a similar calculation by Curci et al. [6], where Wilson loops are also calculated up to order g^4. The revised version of

ref. [6] is now in agreement with our results presented here up to a $1/V$ contribution, which is due to a slightly different contribution of the Haar measure to the effective action (see sect. 2 for a discussion of this point).

In the next two, rather technical, sections, we present the perturbative computation of Wilson loops, average plaquettes and Polyakov lines. Sect. 2 serves to fix our conventions and to discuss the (unsolved) problems of the zero-momentum modes in perturbation theory on finite lattices. Sect. 3 contains our results in analytical form, as far as is possible. In sect. 4, we give the numerical results together with a few applications of the perturbative calculations. Since we have performed the computations on asymmetric hypercubic lattices, we can use the results to discuss zero- as well a finite-temperature effects. For zero temperature, we will discuss the extraction of the coulombic part of the heavy quark potential on finite lattices. At finite temperature, we analyze the high-temperature behaviour of the interacting gluon gas [7] and the order parameter of the deconfinement phase transition [8]. We compare these weak coupling results with MC data for SU(2). As another application, we discuss the usage of the weak coupling expansion in the selection of perturbatively improved operators used in the "improved ratio method" [9, 10] to determine the lattice β-function. Finally, sect. 5 contains our conclusions.

2. Perturbation theory on a finite lattice

2.1. THE EFFECTIVE ACTION

The setup of perturbation theory on a lattice is well known [11]. Therefore, we use this section mainly to fix our notation. Since we want to calculate also some quantities relevant at finite temperature, besides Wilson loops, we will work on an asymmetric lattice of size $V = L^{d-1} \times L_d$. For the sum over the Fourier modes, we use the notation (lattice spacing $a = 1$)

$$\int_p = \frac{1}{V} \sum_{\substack{p \\ (p \neq 0)}} , \tag{2.1}$$

where $p = (p_1, \ldots, p_{d-1}, p_d)$, $p_\mu = (2\pi/L) n_\mu$, $n_\mu = 0, 1, \ldots, L-1$ for $\mu \neq d$ and $p_d = (2\pi/L_d) n_d$, $n_d = 0, 1, \ldots, L_d - 1$. In the sum (2.1), the zero-momentum mode is left out (see below). In the Fourier transforms, we take link variables to live in the middle of the link, plaquette variables to live in the middle of the plaquette and so on, e.g.,

$$A^a_\mu(p) = \sum_x \mathrm{e}^{-ipx - ip_\mu/2} A^a_\mu(x) \tag{2.2}$$

defines the Fourier transform of the gauge field $A^a_\mu(x)$. We use the Wilson action ($Z = \int \prod \mathrm{d}U \exp S$)

$$S = \frac{1}{g^2} \sum_P \mathrm{tr}\,(U_P + U_P^+ - 2) . \tag{2.3}$$

At weak coupling ($U_\mu(x) = \exp\{igA_\mu(x)\}$, $A_\mu(x) = A^a_\mu(x)t^a$) we find the effective action, including gauge fixing (we use the Feynman gauge), Faddeev-Popov determinant and the contribution from the rewriting of the Haar measure $dU_\mu(x)$ in terms of the A_μ's:

$$S_{\text{eff}} = S_0 + gS_1 + g^2S_2 + g^2\bar{S}_2 + g^2S_{\text{FP}} + g^2S_{\text{meas.}}\,. \tag{2.4}$$

S_0 is the term quadratic in the A_μ's:

$$S_0 = -\tfrac{1}{2}\sum_{x,\mu} A^a_\mu(x)(-\Delta)A^a_\mu(x) = -\tfrac{1}{2}\int_p A^a_\mu(-p)D(p)A^a_\mu(p)\,, \tag{2.5}$$

where Δ is the lattice laplacian and

$$D(p) = 4\sum_\rho s^2_\rho(\tfrac{1}{2}p)\,, \tag{2.6}$$

We use the notation $s_\rho(\alpha) = \sin\alpha_\rho$ and $c_\rho(\alpha) = \cos\alpha_\rho$. S_0 is the free part of the action in the perturbation expansion and gives the free gluon propagator

$$\langle A^a_\mu(p)A^b_\nu(k)\rangle_0 = \delta^{ab}\delta_{\mu\nu}V\tilde{\delta}_{p+k,0}D^{-1}(p)\,, \tag{2.7}$$

where $\tilde{\delta}_{p,0}$ is the Kronecker δ modulo 2π.

S_1 gives the three gluon vertex and $S_2 + \bar{S}_2$ the four-gluon vertices from the expansion of the action (2.3). They can be found in ref. [11]. We separated the four-gluon piece with $\bar{S}_2$ given by

$$\bar{S}_2 = \tfrac{1}{24}\sum_x\sum_{\mu,\nu}\operatorname{tr}(\Delta_\mu A_\nu(x) - \Delta_\nu A_\mu(x))^4\,. \tag{2.8}$$

Firstly, $\bar{S}_2$ will give a different N-dependence from S_2 in the results, and secondly, for one-plaquette actions other than the Wilson action, eq. (2.3), $\bar{S}_2$ will have a different coefficient than in (2.8), whereas all the other parts in the expansion (2.4) remain unchanged.

The contribution from the Faddeev-Popov determinant is

$$\begin{aligned} S_{\text{FP}} = {} & -\tfrac{1}{12}NI\sum_{\mu\neq d}\int_p A^a_\mu(-p)A^a_\mu(p) - \tfrac{1}{12}NI_d\int_p A^a_d(-p)A^a_d(p) \\ & -2N\sum_{\mu,\nu}\int_p\int_k A^a_\mu(p-k)A^a_\nu(k-p)\frac{s_\mu(\frac{1}{2}p)s_\nu(\frac{1}{2}k)c_\mu(\frac{1}{2}k)c_\nu(\frac{1}{2}p)}{D(p)D(k)}\,, \end{aligned} \tag{2.9}$$

where I and I_d are defined as

$$\begin{aligned} I &= 4\int_p \frac{s^2_1(\frac{1}{2}p)}{D(p)}\,, \\ I_d &= 4\int_p \frac{s^2_d(\frac{1}{2}p)}{D(p)}\,. \end{aligned} \tag{2.10}$$

For a symmetric lattice ($L_d = L$), we find, using the cubic symmetry,

$$I = I_d = \frac{1}{d}\left(1 - \frac{1}{V}\right) \quad \text{for sym. lattice}. \tag{2.11}$$

The $1/V$ correction arises, since we leave our the zero-momentum mode. In appendix A, we will discuss the changes that occur when one uses a slightly different gauge fixing term. The contribution from the measure finally is

$$S_{\text{meas.}} = -\tfrac{1}{24} N \sum_{x,\mu} (A^a_\mu(x))^2 . \tag{2.12}$$

For reasons not clear to us, Curci et al. [6] use in $S_{\text{meas.}}$ an additional factor of $(1 - 1/V)$. This gives the slight discrepancy in our final results.

In the following, we will also use the notation

$$\Delta_0 = \int_p \frac{1}{D(p)},$$

$$\Delta_1 = \int_p \frac{c_1(p)}{D(p)},$$

$$\Delta_1^d = \int_p \frac{c_d(p)}{D(p)}, \tag{2.13}$$

which denotes the propagators at distance 0, 1 in the directions 1 to $(d-1)$ and 1 in the direction d.

2.2. THE ZERO-MOMENTUM MODES

As can be seen from (2.5), the zero-momentum modes are non-gaussian. The propagator $D^{-1}(p)$ is singular, like p^{-2} at $p = 0$, and on a finite lattice is not suppressed by phase space. They have thus to be treated separately. For LGT's, the zero-momentum modes are not zero-action modes. The action is quartic in the zero-momentum modes, proportional at lowest order to $\sum_{\mu \neq \nu} \text{tr}\,([A_\mu(p=0), A_\nu(p=0)]^2)$. Therefore, they cannot be treated by using collective coordinates, contrary to the case of the O(N) non-linear σ-models [12]. The zero-momentum modes correspond to constant gauge field configurations. It has been argued that, except when they belong to the centre of the gauge group, their contributions to the partition function are highly suppressed [13]. Due to the lack of a better way of treating the zero-momentum modes, we decided, as is usually done [6, 13], to neglect them completely. Thus our momentum sums never include the zero-momentum mode [see (2.1)]. The error introduced in doing so is expected to vanish as $1/V$ in the infinite volume limit.

When the constant gauge fields are centre elements, we simply make an expansion around them instead of around the unit element. However, the centre elements do not contribute to the action and to Wilson loops. Thus, expanding around each centre element gives the same contribution, and therefore gives in the partition

function just an overall multiplicative factor which drops out in the expectation values of Wilson loops. Polyakov lines, on the other hand, are of interest at finite tempeature. There the perturbative regime lies in the deconfined phase where the $Z(N)$ symmetry is sponteneously broken [14]. We assume that it has been aligned to the unit element and thus we have to expand only around it.

3. Wilson loops and Polyakov lines to one loop

We consider planar Wilson loops

$$W(R, T) = \frac{1}{N} \operatorname{tr} \left(\prod_{\ell \in C} U_\ell \right), \tag{3.1}$$

where the path C is a rectangle with sides R in the μ-direction and T in the ν-direction. At weak coupling, the Wilson loop can be expanded as

$$W(R, T) = 1 - g^2 \omega_2 - g^3 \omega_3 - g^4 \omega_4 - g^4 \bar{\omega}_4 + O(g^5) . \tag{3.2}$$

The ω_i are given in appendix B. The expectation value of Wilson loops is then, up to order g^4,

$$\langle W(R, T) \rangle = 1 - g^2 W_2(R, T) - g^4 W_4(R, T) + O(g^6) . \tag{3.3}$$

The lowest-order part is geven by $W_2(R, T) = \langle \omega_2 \rangle_0 = (N^2 - 1)/N \bar{W}_2(R, T)$ with

$$\bar{W}_2(R, T) = \int_p \frac{s_\nu^2(\tfrac{1}{2} pT) S_\mu^2(\tfrac{1}{2} pR)}{D(p)} \left\{ \frac{1}{s_\mu^2(\tfrac{1}{2} p)} + \frac{1}{s_\nu^2(\tfrac{1}{2} p)} \right\} . \tag{3.4}$$

Here $\langle \cdots \rangle_0$ denotes the (connected) expectation value with respect to the quadratic part of the action S_0 given in (2.5). The order g^4 contribution we write as

$$W_4(R, T) = W_{s_1} + W_{\mathrm{I}} + W_{\mathrm{II}} + W_{\mathrm{VP}} + \bar{W}_{\mathrm{VP}} . \tag{3.5}$$

W_{s_1} is the contribution from the "spider" graph (fig. 1):

$$\begin{aligned} W_{s_1} &= \langle \omega_3 S_1 \rangle_0 \\ &= \frac{N^2 - 1}{2} \int_p \int_k \frac{1}{D(p) D(k) D(p+k)} \left[\left\{ \frac{s_\mu^2(\tfrac{1}{2} pR)}{s_\mu(\tfrac{1}{2} p)} s_\nu(\tfrac{1}{2} pT) c_\nu(\tfrac{1}{2} p) s_\mu(\tfrac{1}{2}(2k+p)) \right. \right. \\ &\quad \times \left[\frac{s_\nu(\tfrac{1}{2} pT) s_\nu(\tfrac{1}{2}(2k+p))}{s_\nu(\tfrac{1}{2} p) s_\nu(\tfrac{1}{2} k) s_\nu(\tfrac{1}{2}(p+k))} - \frac{s_\nu(\tfrac{1}{2}(2k+p) T)}{s_\nu(\tfrac{1}{2} k) s_\nu(\tfrac{1}{2}(p+k))} \right] \\ &\quad + 4 \frac{s_\mu(\tfrac{1}{2} pR)}{s_\mu(\tfrac{1}{2} p)} \frac{s_\mu(\tfrac{1}{2} kR)}{s_\mu(\tfrac{1}{2} k)} \frac{s_\nu(\tfrac{1}{2}(p+k) T)}{s_\nu(\tfrac{1}{2}(p+k))} s_\nu(\tfrac{1}{2} pT) c_\nu(\tfrac{1}{2} kT) \\ &\quad \left. \left. \times c_\mu(\tfrac{1}{2}(p+k) R) c_\mu(\tfrac{1}{2}(p+k)) s_\nu(\tfrac{1}{2}(k-p)) \right\} + \{(\mu, R) \leftrightarrow (\nu, T)\} \right] . \end{aligned} \tag{3.6}$$

W_{I} is the expectation value of the non-abelian part of the order g^4 expansion of the Wilson loop. It is

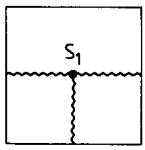

Fig. 1. Order g^4 contribution of the three-gluon vertex S_1 to the Wilson loop expectation values.

$$
\begin{aligned}
W_1 &= \langle \omega_4 \rangle_0 \\
&= -\frac{N^2-1}{3} \Delta_0 \Bigg[\Bigg\{ \int_p \frac{s_\nu^2(\tfrac{1}{2}pT)}{D(p)} \left(\frac{s_\mu^2(\tfrac{1}{2}pR)}{s_\mu^2(\tfrac{1}{2}p)} + \frac{1}{2} \frac{s_\mu(\tfrac{1}{2}pR) s_\mu(\tfrac{1}{2}p(R-2))}{s_\mu^2(\tfrac{1}{2}p)} \right) \Bigg\} \\
&\quad + \{(\mu, R) \leftrightarrow (\nu, T)\} \Bigg] - \frac{N^2-1}{2} \Bigg[\Bigg\{ \int_k \frac{1}{D(k)} \left(\frac{s_\nu^2(\tfrac{1}{2}kT)}{s_\nu^2(\tfrac{1}{2}k)} + \frac{1}{6} \frac{s_\mu^2(\tfrac{1}{2}kR)}{s_\mu^2(\tfrac{1}{2}k)} \right) \\
&\quad \times \int_p \frac{s_\nu^2(\tfrac{1}{2}pT)}{D(p)} \frac{s_\mu^2(\tfrac{1}{2}pR)}{s_\mu^2(\tfrac{1}{2}p)} \Bigg\} + \{(\mu, R) \leftrightarrow (\nu, T)\} \Bigg] \\
&\quad + \frac{N^2-1}{12} \Bigg[\Bigg\{ \Bigg[\int_p \frac{s_\nu^2(\tfrac{1}{2}pT)}{D(p)} \frac{s_\mu^2(\tfrac{1}{2}pR)}{s_\mu^2(\tfrac{1}{2}p)} \Bigg]^2 \Bigg\} + \{(\mu, R) \leftrightarrow (\nu, T)\} \Bigg] \\
&\quad + \tfrac{2}{3}(N^2-1) \int_k \frac{s_\nu^2(\tfrac{1}{2}kT)}{D(k)} \frac{s_\mu^2(\tfrac{1}{2}kR)}{s_\mu^2(\tfrac{1}{2}k)} \int_p \frac{s_\mu^2(\tfrac{1}{2}pR)}{D(p)} \frac{s_\nu^2(\tfrac{1}{2}pT)}{s_\nu^2(\tfrac{1}{2}p)} \\
&\quad + \frac{N^2-1}{4} \int_k \frac{1}{D(k)} \frac{s_\mu^2(\tfrac{1}{2}kR)}{s_\mu^2(\tfrac{1}{2}k)} \int_p \frac{1}{D(p)} \frac{s_\nu^2(\tfrac{1}{2}pT)}{s_\nu^2(\tfrac{1}{2}p)} \\
&\quad + \frac{N^2-1}{32} \int_p \int_k \frac{1}{D(p)D(k)} \Bigg[\Bigg\{ \Bigg[\frac{s_\mu(\tfrac{1}{2}(p+k)R) s_\mu(\tfrac{1}{2}(p-k))}{s_\mu(\tfrac{1}{2}(p+k))} - s_\mu(\tfrac{1}{2}(p-k)R) \Bigg]^2 \\
&\quad \times \frac{s_\nu^2(\tfrac{1}{2}(p+k)T)}{s_\mu^2(\tfrac{1}{2}p) s_\mu^2(\tfrac{1}{2}k)} \Bigg\} + \{(\mu_1 R) \leftrightarrow (\nu, T)\} \Bigg] \\
&\quad + \frac{N^2-1}{6} \int_p \int_k \frac{1}{D(p)D(k)} \Bigg[\Bigg\{ s_\nu^2(\tfrac{1}{2}pT) \frac{s_\mu(\tfrac{1}{2}pR)}{s_\mu(\tfrac{1}{2}p)} \frac{s_\mu(\tfrac{1}{2}kR)}{s_\mu(\tfrac{1}{2}k)} \frac{s_\mu(\tfrac{1}{2}(p+k)R)}{s_\mu(\tfrac{1}{2}(p+k))} \Bigg\} \\
&\quad + \{(\mu, R) \leftrightarrow (\nu, T)\} \Bigg] \\
&\quad - \frac{N^2-1}{6} \int_p \int_k \frac{1}{D(p)D(k)} \Bigg[\Bigg\{ s_\nu^2(\tfrac{1}{2}pT) \frac{s_\mu(\tfrac{1}{2}pR)}{s_\mu(\tfrac{1}{2}p)} \Bigg[\frac{s_\mu(\tfrac{1}{2}p(R-2)) c_\mu(p+k)}{s_\mu(\tfrac{1}{2}p) s_\mu^2(\tfrac{1}{2}k)} \\
&\quad - \frac{s_\mu(\tfrac{1}{2}(p+k)(R-2)) c_\mu(\tfrac{1}{2}k(R+1)+p)}{s_\mu(\tfrac{1}{2}(p+k)) s_\mu^2(\tfrac{1}{2}k)} + \frac{s_\mu(\tfrac{1}{2}p(R-2)) c_\mu(\tfrac{1}{2}p-k)}{s_\mu(\tfrac{1}{2}p) s_\mu(\tfrac{1}{2}k) s_\mu(\tfrac{1}{2}(p+k))} \\
&\quad - \frac{s_\mu(\tfrac{1}{2}k(R-2)) c_\mu(\tfrac{1}{2}(p+k)R+\tfrac{1}{2}k-p)}{s_\mu^2(\tfrac{1}{2}k) s_\mu(\tfrac{1}{2}(p+k))} + \frac{s_\mu(\tfrac{1}{2}(p+k)(R-2)) c_\mu(\tfrac{1}{2}k(R+2)+\tfrac{1}{2}p)}{s_\mu(\tfrac{1}{2}p) s_\mu(\tfrac{1}{2}k) s_\mu(\tfrac{1}{2}(p+k))} \\
&\quad - \frac{s_\mu(\tfrac{1}{2}k(R-2)) c_\mu(\tfrac{1}{2}(p-k)R-p-k)}{s_\mu(\tfrac{1}{2}p) s_\mu^2(\tfrac{1}{2}k)} \Bigg] \Bigg\} + \{\mu, R) \leftrightarrow (\nu, T)\} \Bigg]. \qquad (3.7)
\end{aligned}
$$

W_{II} is the contribution from the abelian part of the expansion of order g^4. We have separated it from W_I since it has a different N-dependence. It is

$$W_{II} = \langle \bar{\omega}_4 \rangle_0 = -\frac{(2N^2-3)(N^2-1)}{6N^2} [\bar{W}_2(R, T)]^2 . \tag{3.8}$$

W_{VP} results from the insertion of the vacuum polarization part $\Pi^{(a)}_{\mu\nu}(p)$ (figs. 2b and 2c), defined in appendix C,

$$W_{VP} = \langle \omega_2(\tfrac{1}{2}S_1^2 + S_2 + S_{FP} + S_{meas.}) \rangle_0$$
$$= \frac{N^2-1}{N} \int_p \frac{s_\nu^2(\frac{1}{2}pT) s_\mu^2(\frac{1}{2}pR)}{D(p)^2} \left\{ \frac{\Pi^{(a)}_{\mu\mu}(p)}{s_\mu^2(\frac{1}{2}p)} - 2\frac{\Pi^{(a)}_{\mu\nu}(p)}{s_\mu(\frac{1}{2}p) s_\nu(\frac{1}{2}p)} + \frac{\Pi^{(a)}_{\nu\nu}(p)}{s_\nu^2(\frac{1}{2}p)} \right\} . \tag{3.9}$$

Finally, $\bar{W}_{VP}$ is the contribution from the insertion of the part $\Pi^{(b)}_{\mu\nu}(p)$ of the vacuum polarization (fig. 2a). For spacelike Wilson loops ($\mu, \nu \neq d$) it is

$$\bar{W}_{VP} = \frac{(2N^2-3)(N^2-1)}{6N^2} I \bar{W}_2(R, T) + \frac{(2N^2-3)(N^2-1)}{3N^2} (I_d - I)$$
$$\times \int_p \frac{s_d^2(\frac{1}{2}p) s_\nu^2(\frac{1}{2}pT) s_\mu^2(\frac{1}{2}pR)}{D(p)^2} \left\{ \frac{1}{s_\mu^2(\frac{1}{2}p)} + \frac{1}{s_\nu^2(\frac{1}{2}p)} \right\} \text{ for } \mu, \nu \neq d , \tag{3.10}$$

while for timelike ones ($\nu = d$) we find

$$\bar{W}_{VP} = \frac{(2N^2-3)(N^2-1)}{12N^2} \int_p \frac{s_d^2(\frac{1}{2}pT) s_\mu^2(\frac{1}{2}pR)}{D(p)} \left\{ \frac{2I}{s_\mu^2(\frac{1}{2}p)} + \frac{I + I_d}{s_d^2(\frac{1}{2}p)} \right\}$$
$$+ \frac{(2N^2-3)(N^2-1)}{3N^2} (I_d - I) \int_p \frac{s_d^2(\frac{1}{2}pT) s_\mu^2(\frac{1}{2}pR)}{D(p)^2} \left\{ \frac{s_d^2(\frac{1}{2}p)}{s_\mu^2(\frac{1}{2}p)} + 1 \right\} . \tag{3.11}$$

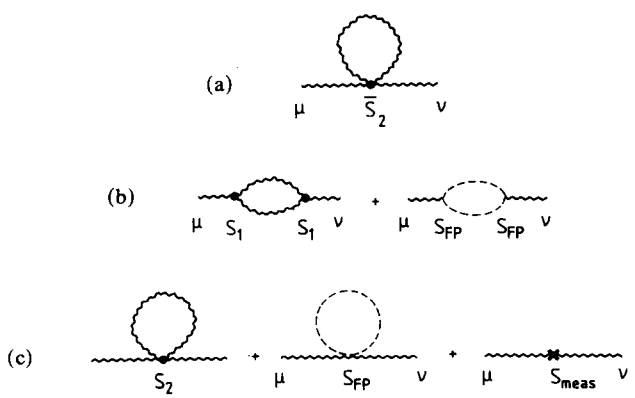

Fig. 2. Order g^2 contributions to the vacuum polarization tensor $\Pi_{\mu\nu}(p)$. Fig. 2a shows the contribution from the four-gluon vertex $\bar{S}_2$, while figs. 2b and 2c contain contributions from the three-gluon vertex S_1, the four-gluon vertex S_2, the Faddeev-Popov term S_{FP} and the measure term S_{meas}. The analytic expressions are given in appendix C.

On a symmetric lattice, the second parts in (3.10) and (3.11) vanish and the contributions for spacelike and timelike loops are, of course, equal. The rather complicated expressions in eqs. (3.6) to (3.11) involving sines and cosines come from explicitly doing the sums over the links along the Wilson loops given in appendix B. Care has to be taken when their denominators vanish, because either p_ρ, k_ρ or $(p+k)_\rho$ equals zero for $\rho=\mu$ or ν. Then the limit, e.g., $p_\mu \to 0$, has to be taken carefully for numerator and denominator. We have checked that this gives the right results by explicitly doing the summation over the links for these "exceptional" momenta.

The average plaquette can, of course, be obtained as the $R=T=1$ Wilson loop. However, in this case, the expression simplifies considerably and we will give it for the spacelike and timelike plaquettes:

$$\left\langle \frac{1}{N} \operatorname{Re}(\operatorname{tr} U_{\mathrm{P}}) \right\rangle_{\text{spacelike}}$$

$$= 1 - \frac{N^2-1}{2N} g^2 I + 2(N^2-1) g^4 \int_p \int_k \frac{c_\nu^2(\tfrac{1}{2}p) s_\mu^2(\tfrac{1}{2}(2k+p))}{D(p)D(k)D(p+k)}$$

$$+ \tfrac{1}{24}(N^2-1) g^4 \{\Delta_0(3\Delta_0 - 2\Delta_1) - \Delta_1(2\Delta_0 + 5\Delta_1)\}$$

$$- 2\frac{N^2-1}{N} g^2 \int_p \frac{1}{D(p)^2} \{s_\nu^2(\tfrac{1}{2}p) \Pi_{\mu\mu}^{(a)}(p) - s_\mu(\tfrac{1}{2}p) s_\nu(\tfrac{1}{2}p) \Pi_{\mu\nu}^{(a)}(p)\}$$

$$+ \frac{(2N^2-3)(N^2-1)}{24N^2} g^4 I^2 - \frac{(2N^2-3)(N^2-1)}{12N^2} g^4 I^2$$

$$- \frac{2(2N^2-3)(N^2-1)}{3N^2} g^4 (I_d - I) \int_p \frac{s_\mu^2(\tfrac{1}{2}p) s_d^2(\tfrac{1}{2}p)}{D(p)^2} \quad \text{for } \mu \neq \nu;\ \mu, \nu \neq d,$$

$$\left\langle \frac{1}{N} \operatorname{Re}(\operatorname{tr} U_{\mathrm{P}}) \right\rangle_{\text{timelike}}$$

$$= 1 - \frac{N^2-1}{4N} g^2 (I + I_d)$$

$$+ (N^2-1) g^4 \int_p \int_k \frac{c_d^2(\tfrac{1}{2}p) s_\mu^2(\tfrac{1}{2}(2k+p)) + c_\mu^2(\tfrac{1}{2}p) s_d^2(\tfrac{1}{2}(2k+p))}{D(p)D(k)D(p+k)}$$

$$+ \frac{N^2-1}{48} g^4 \{2\Delta_0(3\Delta_0 - \Delta_1 - \Delta_1^d) - \Delta_1^d(2\Delta_0 + 4\Delta_1 + \Delta_1^d) - \Delta_1(2\Delta_0 + 4\Delta_1^d + \Delta_1)\}$$

$$- \frac{N^2-1}{N} g^2 \int_p \frac{1}{D(p)^2} \{s_d^2(\tfrac{1}{2}p) \Pi_{\mu\mu}^{(a)}(p) - 2 s_d(\tfrac{1}{2}p) s_\mu(\tfrac{1}{2}p) \Pi_{d\mu}^{(a)}(p) + s_\mu^2(\tfrac{1}{2}p) \Pi_{dd}^{(a)}(p)\}$$

$$+ \frac{(2N^2-3)(N^2-1)}{96N^2} g^4 (I + I_d)^2 - \frac{(2N^2-3)(N^2-1)}{48N^2} g^4 I(I + 3I_d)$$

$$- \frac{(2N^2-3)(N^2-1)}{3N^2} g^4 (I_d - I) \int_p \frac{s_d^2(\tfrac{1}{2}p)}{D(p)^2} \{s_d^2(\tfrac{1}{2}p) + s_\mu^2(\tfrac{1}{2}p)\}. \qquad (3.13)$$

The last two terms in (3.12) and (3.13) come from the four-gluon vertex $\bar{S}_2$ and change their coefficients for other one-plaquette actions.

We finish this section by giving the one-loop expansion for Polyakov lines. A Polyakov line L is the ordered product of the link elements U_e along a direction in the lattice that closes on itself because of the periodic boundary conditions. We take it along the d-direction of the asymmetric lattice. L has an expansion similar to the Wilson loops [(3.5) and appendix B]. For the expectation value up to order g^4, we obtain

$$\begin{aligned}\langle L\rangle = 1 &- \frac{N^2-1}{4N} g^2 L_d \int_p' \frac{1}{D(p)} - \frac{N^2-1}{4N} g^2 L_d \int_p' \frac{\Pi_{dd}^{(a)}(p)}{D(p)^2} \\ &- \frac{N^2-1}{48} g^4 L_d \int_p' \frac{1}{D(p)} \int_k \frac{1-\tilde{\delta}_{k_d,0}}{D(k)} \left(2 - \frac{3}{s_d^2(\frac{1}{2}k)}\right) \\ &- \frac{N^2-1}{32} g^4 L_d \int_p' \int_k \frac{1-\tilde{\delta}_{k_d,0}}{D(k)D(p+k)} \frac{c_d^2(\frac{1}{2}k)}{s_d^2(\frac{1}{2}k)} \\ &+ \frac{(2N^2-3)(N^2-1)}{96N^2} g^4 L_d^2 \left[\int_p' \frac{1}{D(p)}\right]^2 \\ &- \frac{(2N^2-3)(N^2-1)}{48N^2} g^4 L_d (I + I_d) \int_p' \frac{1}{D(p)} . \end{aligned} \tag{3.14}$$

The last term comes from the vacuum polarization insertion $\Pi_{dd}^{(b)}(p)$ and we have used the notation

$$\int_p' = \frac{1}{L^{d-1}} \sum_{\substack{p \\ (p \neq 0)}} \tilde{\delta}_{p_d,0} . \tag{3.15}$$

4. Some numerical results and applications

In the analytic expressions given in the last section, the sums over the momentum modes still have to be carried out. This has to be done numerically. We have evaluated the Wilson loops on symmetric lattices of size L^4 for various L's between 6 and 24. Since the computation involves double sums over momenta k and p, both four-dimensional, the required computer time grows like L^8. All expressions are symmetric under the simultaneous change $p \to 2\pi - p$, $k \to 2\pi - k$. We have used this symmetry to reduce the sum over p in terms of the integers n_μ ($p_\mu = (2\pi/L)n_\mu$) to $0, 1, \ldots, \frac{1}{2}L$. (We have restricted ourseves to even lattice size L.) This reduces the computer time by a factor $[(\frac{1}{2}L+1)/L]^4$ and makes it possible to go up to $L = 24$. While the computation on a 6^4 lattice takes ~3 CPU sec on a CYBER 875, it goes up to ~20 h of CPU time for $L = 24$. The 4th order coefficient $W_4(R, T)$ has pieces with two different N-dependences. Therefore we write

$$W_4(R, T) = (N^2-1)X(R, T) + \frac{(2N^2-3)(N^2-1)}{6N^2} Y(R, T) , \tag{4.1}$$

where in the notation of (3.5)

$$X(R, T) = \frac{1}{N^2-1}(W_{s_1} + W_I + W_{VP}), \tag{4.2}$$

$$Y(R, T) = \frac{6N^2}{(2N^2-3)(N^2-1)}(W_{II} + \bar{W}_{VP}). \tag{4.3}$$

On a symmetric lattice of size $V = L^4$, we obtain for $Y(R, T)$

$$Y(R, T) = -[\bar{W}_2(R, T)]^2 + \tfrac{1}{4}(1 - 1/V)\bar{W}_2(R, T). \tag{4.4}$$

$\bar{W}_2(R, T)$ and $X(R, T)$ are independent of the gauge group. They are listed in tables 1 and 2 for selected Wilson loops on lattices of various sizes. Table 1 contains the Wilson loops on an 8^4 and 12^4 lattice, as well as the corresponding loops of twice the size on a 16^4 and 24^4 lattice.

Table 2 illustrates the dependence of small Wilson loops on the lattice size. The finite size effects grow with the size of the Wilson loops and seem to decrease roughly as $1/V$. It would take too much space to list all our numbers. Interested readers can obtain them from the authors. In the following, we will discuss some applications of our perturbative results.

4.1. THE RATIO METHOD

Ratios of Wilson loops combined in such a way that the corner and self-mass contributions cancel, can be used to study the non-perturbative lattice β-function of the SU(N) gauge theories. The basic idea of the method was already proposed several years ago by Creutz [15]. In the ratio method, ratios of Wilson loops, like

$$R_2(i_1, i_2, i_3, i_4) = \frac{W(i_1, i_2)}{W(i_3, i_4)}, \qquad i_1 + i_2 = i_3 + i_4,$$

$$R_4(i_1, i_2, \ldots, i_8) = \frac{W(i_1, i_2)\,W(i_3, i_4)}{W(i_5, i_6)\,W(i_7, i_8)}, \qquad i_1 + \cdots + i_4 = i_5 + \cdots + i_8, \tag{4.5}$$

are compared with ratios formed from loops twice as large. These ratios satisfy the homogeneous renormalization group equation

$$R_2(2i_1, \ldots, 2i_4, g^2, L) = R_2(i_1, \ldots, i_4, g'^2, \tfrac{1}{2}L), \tag{4.6}$$

which determines the change in g^2 necessary to vary the lattice spacing by a factor of 2 [$g^2(a) \to g'^2(2a)$]. (A similar equation is valid for R_n, $n = 4 \cdots$).

In eq. (4.6), the lattice volume is scaled together with the correlation length to reduce the finite size effects. The basic ratios defined in eq. (4.5) may be sufficient to study the non-perturbative β-function at intermediate correlation lengths. However, a tree-level perturbative calculation already shows that in practice, i.e., in a MC simulation on finite lattices where only small Wilson loops can be measured,

TABLE 1a

Coefficients of the perturbative expansion of Wilson loops on a 8^4 lattice and of corresponding Wilson loops of twice the size on a 16^4 lattice

R	T	8^4 lattice		16^4 lattice	
		$\bar{W}_2(R, T)$	$X(R, T)$	$\bar{W}_2(2R, 2T)$	$X(2R, 2T)$
1	1	0.124969	$-1.03246 \cdot 10^{-4}$	0.342297	$-6.27874 \cdot 10^{-3}$
1	2	0.215433	$-1.58383 \cdot 10^{-3}$	0.559537	$-2.72088 \cdot 10^{-3}$
2	2	0.341778	$-6.27233 \cdot 10^{-3}$	0.814820	$-6.91343 \cdot 10^{-2}$
1	3	0.300224	$-5.42197 \cdot 10^{-3}$	0.770462	$-6.29591 \cdot 10^{-2}$
2	3	0.451484	$-1.47960 \cdot 10^{-2}$	1.051051	−0.128285
3	3	0.573010	$-2.81174 \cdot 10^{-2}$	1.297682	−0.208902
1	4	0.383725	$-1.15742 \cdot 10^{-2}$	0.980396	−0.113325
2	4	0.556886	$-2.69621 \cdot 10^{-2}$	1.283756	−0.205021
3	4	0.686217	$-4.53413 \cdot 10^{-2}$	1.537299	−0.307195
4	4	0.802559	$-6.72169 \cdot 10^{-2}$	1.779707	−0.425781

$\bar{W}_2(R, T)$ is the N-independent factor of the $O(g^2)$ contribution and $(N^2-1)X(R, T)$ is the non-trivial $O(g^4)$ contribution defined in eq. (4.2).

TABLE 1b

Same as table 1a but on 12^4 and 24^4 lattices respectively

R	T	12^4 lattice		24^4 lattice	
		$\bar{W}_2(R, T)$	$X(R, T)$	$\bar{W}_2(2R, 2T)$	$X(2R, 2T)$
1	1	0.124994	$-1.01812 \cdot 10^{-4}$	0.342322	$-6.27861 \cdot 10^{-3}$
1	2	0.215538	$-1.58180 \cdot 10^{-3}$	0.559644	$-2.72161 \cdot 10^{-2}$
2	2	0.342227	$-6.27854 \cdot 10^{-3}$	0.815269	$-6.91966 \cdot 10^{-2}$
1	3	0.300491	$-5.42873 \cdot 10^{-3}$	0.770727	$-6.29988 \cdot 10^{-2}$
2	3	0.452603	$-1.48542 \cdot 10^{-2}$	1.052154	−0.128523
3	3	0.575748	$-2.83508 \cdot 10^{-2}$	1.300350	−0.209676
1	4	0.384295	$-1.16184 \cdot 10^{-2}$	0.980943	−0.113455
2	4	0.559226	$-2.71843 \cdot 10^{-2}$	1.286003	−0.205689
3	4	0.691777	$-4.60265 \cdot 10^{-2}$	1.542625	−0.309157
4	4	0.813459	$-6.89345 \cdot 10^{-2}$	1.790061	−0.430382
1	5	0.467773	$-2.01219 \cdot 10^{-2}$	1.190904	−0.178564
2	5	0.664681	$-4.31870 \cdot 10^{-2}$	1.518898	−0.300741
3	5	0.805455	$-6.78589 \cdot 10^{-2}$	1.782925	−0.427337
4	5	0.931381	$-9.60886 \cdot 10^{-2}$	2.034280	−0.570339
5	5	1.051981	−0.128408	2.281021	−0.731622
1	6	0.551110	$-3.09260 \cdot 10^{-2}$	1.400745	−0.258316
2	6	0.769604	$-6.28172 \cdot 10^{-2}$	1.751323	−0.413661
3	6	0.918007	$-9.37974 \cdot 10^{-2}$	2.022215	−0.564242
4	6	1.047429	−0.127473	2.276799	−0.729165
5	6	1.169836	−0.164877	2.525252	−0.911505
6	6	1.288525	−0.206188	2.770278	−1.111840

TABLE 2

Coefficients of the perturbative expansion of small Wilson loops for various lattice sizes

Contribution	8^4	10^4	12^4	16^4	20^4	24^4
$\bar{W}_2(1,1)$	0.124929	0.124988	0.124994	0.124998	0.124999	0.125000
$X(1,1)$	$-1.03246 \cdot 10^{-4}$	$-1.02208 \cdot 10^{-4}$	$-1.01812 \cdot 10^{-4}$	$-1.01544 \cdot 10^{-4}$	$-1.01465 \cdot 10^{-4}$	$-1.01434 \cdot 10^{-4}$
$\bar{W}_2(1,2)$	0.215433	0.215511	0.215538	0.215555	0.215559	0.215561
$X(1,2)$	$-1.58383 \cdot 10^{-3}$	$-1.58245 \cdot 10^{-3}$	$-1.58180 \cdot 10^{-3}$	$-1.58130 \cdot 10^{-3}$	$-1.58114 \cdot 10^{-3}$	$-1.58107 \cdot 10^{-3}$
$\bar{W}_2(2,2)$	0.341778	0.342113	0.342227	0.342297	0.342315	0.342322
$X(2,2)$	$-6.27233 \cdot 10^{-3}$	$-6.27754 \cdot 10^{-3}$	$-6.27854 \cdot 10^{-3}$	$-6.27874 \cdot 10^{-3}$	$-6.27866 \cdot 10^{-3}$	$-6.27861 \cdot 10^{-3}$
$\bar{W}_2(1,3)$	0.300224	0.300425	0.300491	0.300531	0.300542	0.300545
$X(1,3)$	$-5.42197 \cdot 10^{-3}$	$-5.42757 \cdot 10^{-3}$	$-5.42873 \cdot 10^{-3}$	$-5.42912 \cdot 10^{-3}$	$-5.42914 \cdot 10^{-3}$	$-5.42913 \cdot 10^{-3}$
$\bar{W}_2(2,3)$	0.451484	0.452329	0.452603	0.452768	0.452811	0.452826
$X(2,3)$	$-1.47960 \cdot 10^{-2}$	$-1.48416 \cdot 10^{-2}$	$-1.48542 \cdot 10^{-2}$	$-1.48607 \cdot 10^{-2}$	$-1.48620 \cdot 10^{-2}$	$-1.48624 \cdot 10^{-2}$
$\bar{W}_2(3,3)$	0.573010	0.575091	0.575748	0.576133	0.576232	0.576267
$X(3,3)$	$-2.81174 \cdot 10^{-2}$	$-2.82982 \cdot 10^{-2}$	$-2.83508 \cdot 10^{-2}$	$-2.83792 \cdot 10^{-2}$	$-2.83858 \cdot 10^{-2}$	$-2.83879 \cdot 10^{-2}$

these simple observables are not sufficient to connect the non-perturbative regime with the known perturbative behaviour of the β-function at large correlation length:

$$-a\frac{\mathrm{d}g(a)}{\mathrm{d}a} = -b_0 g^3 - b_1 g^5 + \mathrm{O}(g^7)\,, \tag{4.7}$$

with

$$b_0 = \frac{11N}{48\pi^2}, \qquad b_1 = \frac{34}{3}\left(\frac{N}{16\pi^2}\right)^2.$$

While eq. (4.7) leads to a constant shift in g^2 necessary to change the lattice spacing by a factor of 2,

$$\Delta g^{-2} = 2b_0 \log 2\,, \tag{4.8}$$

the ratios, eq. (4.5), would lead to a shift which diverges in the limit $g^2 \to 0$. As the ratios $R_j(i_1, i_2, \ldots)$ and $R_j(2i_1, 2i_2, \ldots)$ have different perturbative coefficients in order g^2:

$$R_j(ni_1, ni_2, \ldots) = 1 - a_j(ni_1, ni_2, \ldots)g^2\,, \qquad n = 1, 2\,, \tag{4.9}$$

one finds from eq. (4.6)

$$\Delta g^{-2} = \left(\frac{a_j(2i_1, 2i_2, \ldots)}{a_j(i_1, i_2, \ldots)} - 1\right)g^{-2}. \tag{4.10}$$

This problem has been observed in renormalization group studies of the O(N) spin models [9, 16], and it has been shown in ref. [9] that a successful way to proceed is to use, instead of the simple operators eq. (4.5), improved observables which already show a better weak coupling behaviour on finite lattices and for finite loop sizes, i.e., the O(g^2) coefficient is the same when the loops involved in these observables are scaled by a factor of 2.These improved ratios are given by

$$R_{jk} = R_j(i_1, i_2, \ldots) + \alpha R_k(l_1, l_2, \ldots)\,, \tag{4.11}$$

with

$$\alpha = \frac{a_j(2i_1, 2i_2, \ldots) - a_j(i_1, i_2, \ldots)}{a_k(2l_1, 2l_2, \ldots) - a_k(l_1, l_2, \ldots)}.$$

The shift Δg^{-2} for these ratios can be calculated in the limit $g^2 \to 0$ using our one-loop results for the Wilson loops given in tables 1 and 2. Of course, these tree-level improved ratios will not give the exact one-loop result eq. (4.8) either, but will scatter around this value as the lattice artefacts still influence the finite loops involved in the ratios. However, neglecting observables which contain very small loops will improve the results further. In figs. 3a and 3b, we show the matching predictions $\Delta(6/g^2)$ in the case of SU(3) obtained for improved ratios comparing loops measured on 16^4 and 8^4 lattices (fig. 3a) and 24^4 and 12^4 lattices (fig. 3b) respectively. These

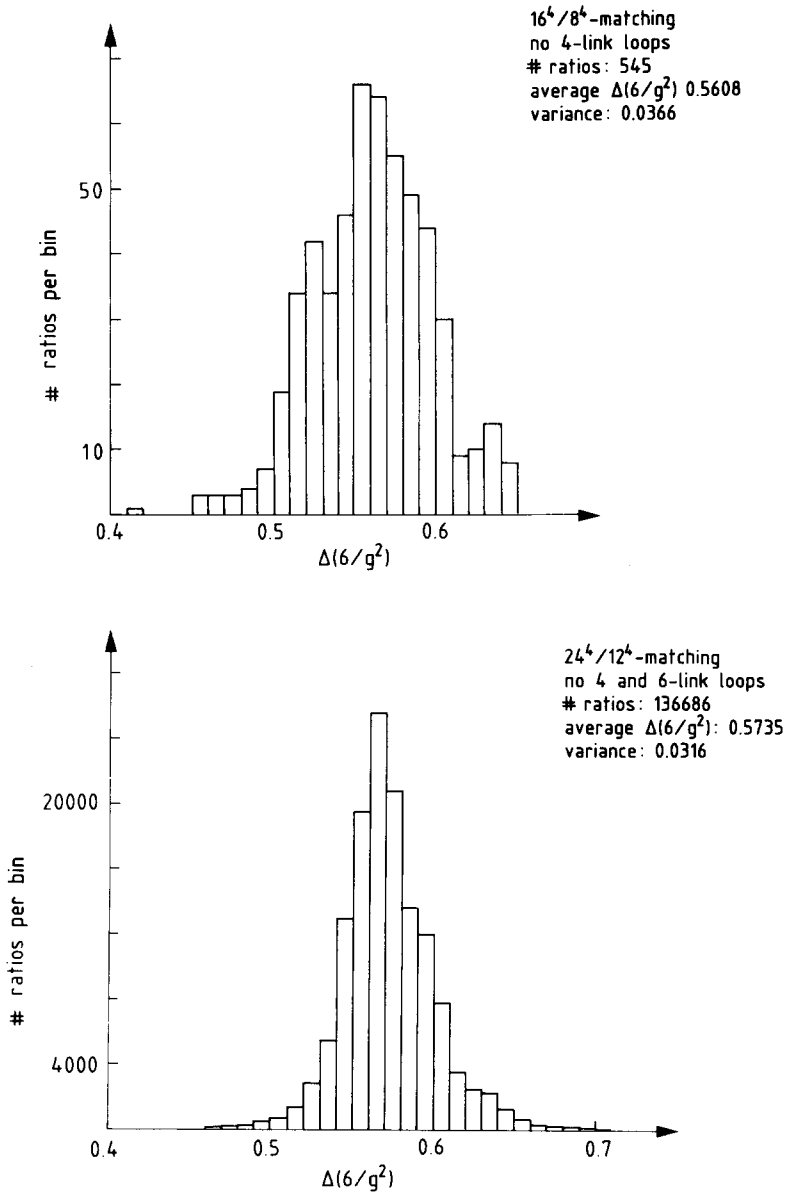

Fig. 3. Asymptotic ($g^2 \to 0$) behaviour of the shift $\Delta(6/g^2)$ obtained from tree-level improved ratios of SU(3) Wilson loops. Figs. 3a and 3b show the distribution of matching predictions when ratios $R_{jk}(i_1, i_2, \ldots)$ calculated on a $(\frac{1}{2}L)^4$ lattice are compared with corresponding ratios $R_{jk}(2i_1, 2i_2, \ldots)$ on an $(L)^4$ lattice. To be compatible with the MC analysis of ref. [10], only ratios where the total area of the loops in the denominator minus the area in the numerator is non-zero (positive) and the mixing coefficient α is in the range $\alpha \in (0, 3)$ have been analyzed. In fig. 3a, $L = 16$ and only ratios which contain loops with perimeter larger than 4 have been considered. In fig. 3b, $L = 24$ and loops with perimeter larger than 6 are used in the analysis.

figures show that leaving out observables formed from very small loops systematically improves the prediction for the asymptotic shift $\Delta(6/g^2)$ and reduces the scattering of the individual observables around the exact value $\Delta(6/g^2) = 0.579$ for SU(3). The distribution of asymptotic shifts shown in fig. 3b involves 136 686 observables formed from loops with perimeter larger than 6, which gave an average shift $\Delta(6/g^2) = 0.5735$ with a variance of 0.0316.

Using our one-loop results we can, however, go one step further and consider "one-loop improved" observables which already yield the exact one-loop prediction, eq. (4.8), for loops of any finite size. This can be achieved by combining three basic ratios of the type defined in eq. (4.5):

$$R_{ijk} = R_i + \alpha R_j + \beta R_k . \tag{4.12}$$

The mixing coefficients α, β can be determined using the one-loop results given in tables 1 and 2. These observables have been used in ref. [10] to study the SU(3) lattice β-function.

4.2. THE LATTICE COULOMB POTENTIAL

At short distances, compared to the correlation length, the heavy quark potential is dominated by the coulombic part resulting from gluon exchange. This should be seen in MC simulations at larger values of $\beta = 2N/g^2$. However, on finite lattices, the Coulomb potential is distorted by lattice artefacts. We can get an idea of this lattice effect by computing the potential from our weak coupling expansion of Wilson loops in the same way that it is done in MC simulations. One builds finite-T approximants $V_T(R)$ of the heavy quark potential. We obtain their perturbative expansion as

$$\begin{aligned} V_T(R) = \log\left[\frac{\langle W(R, T-1)\rangle}{\langle W(R, T)\rangle}\right] &= g^2 \frac{N^2-1}{N}[\bar{W}_2(R, T) - \bar{W}_2(R, T-1)] \\ &+ g^4(N^2-1)[X(R, T) - X(R, T-1) \\ &+ \tfrac{1}{6}(\bar{W}_2(R, T)^2 - \bar{W}_2(R, T-1)^2)] \\ &+ g^4 \frac{(2N^2-3)(N^2-1)}{24N^2}\left(1 - \frac{1}{V}\right)[\bar{W}_2(R, T) - \bar{W}_2(R, T-1)] . \end{aligned} \tag{4.13}$$

For large distances, $R \gg a$, the lowest-order part (one-gluon exchange) is just the usual Coulomb potential plus a self-energy term:

$$V^{(2)}(R) = \lim_{T\to\infty} V_T^{(2)}(R) = V_{\text{self}} - g^2 \frac{N^2-1}{N}\frac{C}{R}, \qquad R \gg a , \tag{4.14}$$

with $C = 1/8\pi = 0.0398$. For smaller distances (and T's) this is distorted by lattice effects. If we still assume the form (4.14) and extract C from the finite-T approximants $V_T^{(2)}(R) - V_T^{(2)}(R-1)$, we find the values listed in table 3. We can see that

TABLE 3

The "Coulomb" coefficient C and logarithm of the scale parameter M for SU(3) extracted from the weak coupling expansion of finite-T approximants $V_T(R) - V_T(R-1)$ on lattices of size 16^4 and 24^4

R	T	C		log M for SU(3)	
		16^4	24^4	16^4	24^4
2	6	0.0437	0.0438	4.288	4.289
	7	0.0434	0.0435	4.281	4.282
	8	0.0431	0.0434	4.278	4.278
	10		0.0432		4.275
	12		0.0432		4.275
3	6	0.0438	0.0490	4.277	4.282
	7	0.0468	0.0477	4.254	4.261
	8	0.0458	0.0470	4.239	4.247
	10		0.0463		4.232
	12		0.0459		4.225
4	6	0.0491	0.0511	4.330	4.338
	7	0.0453	0.0480	4.311	4.323
	8	0.0427	0.0462	4.289	4.305
	10		0.0443		4.278
	12		0.0432		4.263
6	6	0.0573	0.0660	4.296	4.293
	7	0.0448	0.0560	4.373	4.362
	8	0.0358	0.0500	4.407	4.389
	10		0.0435		4.387
	12		0.0396		4.367

in the weak coupling limit, $V_T(R)$ approaches the limit $T \to \infty$ much slower than measured in MC simulations at $g^2 \sim O(1)$. We can clearly see lattice and finite size effects, the latter becoming smaller when the size is increased as it should be. But these effects are not overwhelming, which might explain why fits of the form Coulomb + linear to the potential determined in MC simulations work rather well (for recent measurement of the SU(3) potential see, e.g. [17]). Close to the continuum limit, the order g^4 contributions to the potential can be absorbed into the definition of a running coupling constant and a scale parameter. If we do this for our lattice potential, i.e., if we write [for SU(3)]:

$$V_T(R) = g^2 V_T^{(2)}(R) + g^4 V_T^{(4)}(R)$$

$$= V_{\text{self}} - \tfrac{8}{3} g_T^2(R) \frac{C_T(R)}{R}, \tag{4.15}$$

with $C_T(R)$ determined from lowest order and

$$g_T^2(R) = g^2 \left(1 + \frac{11}{16\pi^2} g^2 \log (R M_T(R))^2 \right), \tag{4.16}$$

we find for $\log M_T(R)$ the values also listed in table 3. For $T \to \infty$ and $R \gg a$, $M_T(R)$ should become independent of R and take on the value [18]

$$\log M = \lim_{T\to\infty} \log M_T = \log \frac{\Lambda_P}{\Lambda_L} = 4.407 . \tag{4.17}$$

Already at the distances (and T) considered, the agreement is quite good.

4.3. INTERNAL ENERGY OF THE GLUON GAS

With the definition of the average plaquette as

$$P = 1 - \frac{1}{N} \langle \mathrm{tr}\, U_P \rangle , \tag{4.18}$$

the internal energy of the gluon gas can be obtained as [7]

$$\varepsilon = 6N \left\{ \frac{1}{g^2} (P_\sigma - P_\tau) + c'_\sigma (P_{\mathrm{sym}} - P_\sigma) + c'_\tau (P_{\mathrm{sym}} - P_\tau) \right\} , \tag{4.19}$$

where [19]

$$c'_\sigma = 4N \left\{ \frac{N^2-1}{32N^2} \times 0.586844 + 0.000499 \right\} ,$$

$$c'_\tau = 4N \left\{ -\frac{N^2-1}{32N^2} \times 0.586844 + 0.005306 \right\} , \tag{4.20}$$

and P_σ, P_τ are the average plaquettes in space-space and space-time directions respectively. P_{sym} is the average plaquette on a symmetric lattice. At $g^2 = 0$, one has a gas of non-interacting gluons, and the internal energy should obey the Stefan-Boltzmann law ($T = 1/L_4$)

$$\varepsilon_{\mathrm{SB}} = (N^2-1)\tfrac{1}{15}\pi^2 T^4 . \tag{4.21}$$

But on finite lattices, the lattice artefacts cause (sometimes large) corrections to this law [20]. Away from $g^2 = 0$, other corrections due to the interactions between the gluons appear. For small g^2, these corrections can be computed in perturbation theory. We find the necessary expansion of P_σ and P_τ as

$$P_{\sigma,\tau} = g^2 \frac{N^2-1}{N} P^{(2)}_{\sigma,\tau} + g^4 (N^2-1) P^{(4a)}_{\sigma,\tau}$$

$$+ g^4 \frac{(2N^2-3)(N^2-1)}{N^2} P^{(4b)}_{\sigma,\tau} + \mathrm{O}(g^6) , \tag{4.22}$$

The coefficients $P^{(i)}_{\sigma,\tau}$ are N-independent and given for various asymmetric lattices in table 4. We have computed the internal energy for SU(2) on a lattice of size $10^3 \times 3$ as a function of the temperature $T = (L_4 a)^{-1}$, using the one-loop relation

TABLE 4

Coefficients of the perturbative expansion of space-space (P_σ) and space-time (P_τ) plaquettes on various asymmetric lattices of size $L^3 \times L_4$: the perturbative expansion is defined in eq. (4.18)

	L_4	$P_\sigma^{(2)}$	$P_\sigma^{(4a)}$	$P_\sigma^{(4b)}$	$P_\tau^{(2)}$	$P_\tau^{(4a)}$	$P_\tau^{(4b)}$
8^3	2	0.130788	$-2.94025 \cdot 10^{-4}$	$2.77555 \cdot 10^{-3}$	0.118968	$-9.1229 \cdot 10^{-5}$	$2.43426 \cdot 10^{-3}$
	3	0.126082	$-1.41533 \cdot 10^{-4}$	$2.63080 \cdot 10^{-3}$	0.123755	$-9.4764 \cdot 10^{-5}$	$2.57120 \cdot 10^{-3}$
	4	0.125239	$-1.11582 \cdot 10^{-4}$	$2.60906 \cdot 10^{-3}$	0.124639	$-1.02366 \cdot 10^{-4}$	$2.59421 \cdot 10^{-3}$
	8	0.124969	$-1.03246 \cdot 10^{-4}$	$2.60290 \cdot 10^{-3}$	0.124969	$-1.03246 \cdot 10^{-4}$	$2.60290 \cdot 10^{-3}$
10^3	2	0.130868	$-3.21020 \cdot 10^{-4}$	$2.77876 \cdot 10^{-3}$	0.119007	$-7.9176 \cdot 10^{-5}$	$2.43609 \cdot 10^{-3}$
	3	0.126135	$-1.46509 \cdot 10^{-4}$	$2.63282 \cdot 10^{-3}$	0.123781	$-8.9412 \cdot 10^{-5}$	$2.57250 \cdot 10^{-3}$
	4	0.125279	$-1.11771 \cdot 10^{-4}$	$2.61056 \cdot 10^{-3}$	0.124659	$-9.9834 \cdot 10^{-5}$	$2.59520 \cdot 10^{-3}$
	5	0.125080	$-1.04485 \cdot 10^{-4}$	$2.60571 \cdot 10^{-3}$	0.124870	$-1.02424 \cdot 10^{-4}$	$2.60054 \cdot 10^{-3}$
	10	0.124988	$-1.02208 \cdot 10^{-4}$	$2.60365 \cdot 10^{-3}$	0.124988	$-1.02208 \cdot 10^{-4}$	$2.60365 \cdot 10^{-3}$
12^3	2	0.130903	$-3.41437 \cdot 10^{-4}$	$2.78018 \cdot 10^{-3}$	0.119025	$-7.1215 \cdot 10^{-5}$	$2.43689 \cdot 10^{-3}$
	3	0.126159	$-1.50877 \cdot 10^{-4}$	$2.63371 \cdot 10^{-3}$	0.123793	$-8.5986 \cdot 10^{-5}$	$2.57308 \cdot 10^{-3}$
	4	0.125296	$-1.12495 \cdot 10^{-4}$	$2.61122 \cdot 10^{-3}$	0.124668	$-9.8312 \cdot 10^{-5}$	$2.59564 \cdot 10^{-3}$
	5	0.125094	$-1.04318 \cdot 10^{-4}$	$2.60624 \cdot 10^{-3}$	0.124877	$-1.01579 \cdot 10^{-4}$	$2.60089 \cdot 10^{-3}$
	6	0.125034	$-1.02490 \cdot 10^{-4}$	$2.60479 \cdot 10^{-3}$	0.124942	$-1.02186 \cdot 10^{-4}$	$2.60254 \cdot 10^{-3}$
	12	0.124994	$-1.01812 \cdot 10^{-4}$	$2.60392 \cdot 10^{-3}$	0.124994	$-1.01812 \cdot 10^{-4}$	$2.60392 \cdot 10^{-3}$

between a, Λ_L and g^2. Only the first term in eq. (4.19) contributes to O(1). On a finite lattice, this contribution differs slightly from the corresponding ideal Bose gas, with $2(N^2-1)$ degrees of freedom [20]. We find

$$\left(\frac{\varepsilon}{T^4}\right)_{SU(N)} = \left(\frac{\varepsilon}{T^4}\right)_{Bose}\left(1-\frac{1}{4}\left(\frac{L_4}{L}\right)^3+\frac{1}{4}\left(\frac{L_4}{L}\right)^4\right)+O(g^2)\,. \tag{4.23}$$

In fig. 4, we show this lowest-order term and the $O(g^2)$ corrections together with MC data from ref. [7]. As can be seen, the agreement between the MC data and the weak coupling expansion at high temperature is excellent. We checked that the same is true for a comparison of our weak coupling results with the high temperature tail of the SU(3) gluon gas [21].

4.4. POLYAKOV LINES

Finally, we want to give the perturbative expansion of Polyakov lines:

$$\langle L\rangle = 1-g^2\frac{N^2-1}{N}Q^{(2)}-g^4(N^2-1)Q^{(4a)}-g^4\frac{(2N^2-3)(N^2-1)}{N^2}Q^{(4b)}+O(g^6)\,. \tag{4.24}$$

The N-independent coefficients $Q^{(i)}$ are listed in table 5 for lattices of spatial size 8, 10 and 12, and various extensions in the time (4−) direction. Polyakov lines are used as an order parameter in the investigation of the finite temperature deconfinement transition. However, because of the perturbative contributions, they are not

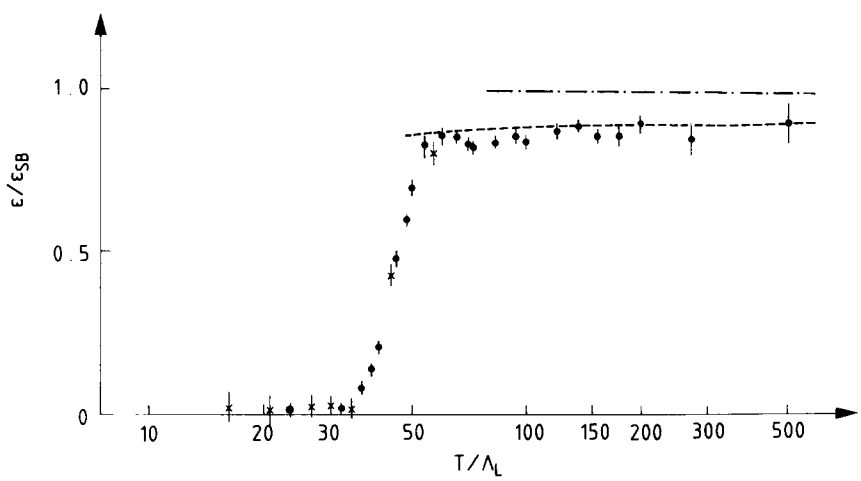

Fig. 4. Comparison of the perturbative corrections of $O(g^2)$ to the high-temperature limit of a gluon gas with SU(2) MC data on a finite lattice of size $10^3\times 3$. The MC data are taken from ref. [7]. They are normalized to the energy density of an ideal Bose gas on a lattice of the same size [20]) (ε_{SB}). The O(1) perturbative result for the SU(2) gluon gas (dashed-dotted curve) agrees with ε_{SB} up to $(L_4/L)^3$ corrections. The broken line shows the $O(g^2)$ corrections due to one-gluon exchange.

TABLE 5

Coefficients of the perturbative expansion of the Polyakov line L on various asymmetric latticesof size $L^3 \times L_4$: the perturbative expansion is defined in eq. (4.24)

	L_4	$Q^{(2)}$	$Q^{(4a)}$	$Q^{(4b)}$
8^3	2	0.112303	$1.51970 \cdot 10^{-3}$	$2.35148 \cdot 10^{-3}$
	3	0.168454	$3.75130 \cdot 10^{-3}$	$2.21955 \cdot 10^{-3}$
	4	0.224606	$3.51234 \cdot 10^{-3}$	$9.23619 \cdot 10^{-4}$
	5	0.280757	$1.12068 \cdot 10^{-3}$	$-1.45281 \cdot 10^{-3}$
10^3	2	0.115100	$7.74240 \cdot 10^{-4}$	$2.35791 \cdot 10^{-3}$
	3	0.172650	$2.76862 \cdot 10^{-3}$	$2.15562 \cdot 10^{-3}$
	4	0.230200	$4.03790 \cdot 10^{-3}$	$7.33498 \cdot 10^{-4}$
	5	0.287750	$1.88110 \cdot 10^{-3}$	$-1.82289 \cdot 10^{-3}$
	6	0.345300	$-2.24471 \cdot 10^{-3}$	$-5.49182 \cdot 10^{-3}$
12^3	2	0.116971	$-1.31722 \cdot 10^{-4}$	$2.36045 \cdot 10^{-3}$
	3	0.175457	$3.59013 \cdot 10^{-3}$	$2.10927 \cdot 10^{-3}$
	4	0.233942	$4.32825 \cdot 10^{-3}$	$6.00189 \cdot 10^{-4}$
	5	0.292428	$2.52525 \cdot 10^{-3}$	$-2.07984 \cdot 10^{-3}$
	6	0.350913	$-1.63369 \cdot 10^{-3}$	$-5.90875 \cdot 10^{-3}$
	7	0.409399	$-7.51596 \cdot 10^{-3}$	$-1.08807 \cdot 10^{-2}$

functions of the physical temperature alone, but also depend on the extension L_4 of the lattice in the time direction. This is due to the self-energy contribution of the static quark source used as order parameter. Elimination of this self-energy term is necessary to obtain an order parameter which is a function of the temperature alone [9], and would allow the extraction of critical exponents for the deconfinement transition. We checked that the subtraction of the perturbative part (4.24) from MC measurements for SU(2) on $10^3 \times L_4$ lattices brings the $L_4 = 3$ and $L_4 = 4$ results onto a universal curve.

5. Conclusions

We have analyzed the one-loop perturbative expansion of planar Wilson loops and the Polyakov lines on finite asymmetric lattices. The agreement of our perturbative results for Wilson loops with those of ref. [6] gives confidence in the final numbers obtained from the rather involved calculation. Although the zero-momentum modes have been treated in a rather naive way, the solution of this problem is expected to give $O(1/V)$ to the results presented here. This, however, will not affect the comparison of the weak coupling expansion with MC data. This comparison works well for the energy density of a gluon gas at high temperature. The Coulomb part of the heavy quark potential can be reproduced quite well by the weak coupling approximants on a finite lattice and supports the validity of fits of the type "Coulomb + linear term" used to extract the string tension from MC data.

What we consider most important, however, is the possibility to construct, from the present results, one-loop improved observables which satisfy the homogeneous renormalization group equation and yield the correct weak coupling solution of this equation. This allows a study of the lattice β-function on finite lattices by operators constructed from loops of finite size which are free from lattice artefacts to order g^4, and smoothly connect the perturbative and non-perturbative regimes.

We thank P. Hasenfratz for many helpful discussions and suggestions. We are indebted to C.P. Korthals-Altes for discussions on the problem of gauge fixing on finite lattices and the zero-momentum modes in LGT. We would also like to thank R. Trippicione for a clarifying discussion on the computations in ref. [6].

Appendix A

GAUGE FIXING

For the gauge fixing term

$$S_{\mathrm{GF}} = -\tfrac{1}{2}\sum_x (G^a(x))^2 , \tag{A.1}$$

we have taken

$$G^a(x) = \sum_\mu \bar{\Delta}_\mu A^a_\mu(x) \tag{A.2}$$

$[\bar{\Delta}_\mu f(x) = f(x) - f(x-\hat{\mu})]$. For the use of BRS transformations to discuss Slavnov-Taylor identities on the lattice, it is more convenient to use a slightly different gauge fixing term [22]:

$$G'^a(x) = \sum_\mu \bar{\Delta}_\mu H^a_\mu(x) , \tag{A.3}$$

where

$$H_\mu(x) = \frac{1}{2ig}(U_\mu(x) - U^+_\mu(x)) = A_\mu(x) - \tfrac{1}{6}g^2 A^3_\mu(x) + \mathrm{O}(g^4) . \tag{A.4}$$

This introduces a new four-gluon term in the effective action:

$$\delta S'_{\mathrm{GF}} = \tfrac{1}{3}g^2 \sum_x \sum_{\mu,\nu} \mathrm{tr}\,[\bar{\Delta}_\mu A_\mu(x) \bar{\Delta}_\nu A^3_\nu(x)] . \tag{A.5}$$

It also gives an additional term to the Faddeev-Popov determinant

$$\delta S_{\mathrm{FP}} = -\frac{2N^2-3}{12N} g^2 I \sum_{\mu \neq d} \int_p A^a_\mu(-p) A^a_\mu(p) - \frac{2N^2-3}{12N} g^2 I_d \int_p A^a_d(-p) A^a_d(p) . \tag{A.6}$$

To the order we are considering, both contributions enter our results only through a change in the vacuum polarization:

$$\delta\Pi_{\mu\nu}(p)=\frac{2(2N^2-3)}{3N}\,g^2\Delta_0 s_\mu(\tfrac{1}{2}p)s_\nu(\tfrac{1}{2}p)\,. \tag{A.7}$$

This is a purely longitudinal contribution and one easily checks that it does not contribute to the expectation value of gauge invariant objects.

Appendix B

EXPANSION OF WILSON LOOPS TO $O(g^4)$

Making repeated use of the Baker-Hausdorf formula

$$\begin{aligned} e^X e^Y = \exp\{&X+Y+\tfrac{1}{2}[X,Y]+\tfrac{1}{12}[X,[X,Y]]+\tfrac{1}{12}[[X,Y],Y] \\ &+\text{commutators involving 4 } X \text{ and } Y+\cdots\}\,, \end{aligned} \tag{B.1}$$

we find

$$\begin{aligned} \prod_{\ell\in C} U_\ell = \exp\Big\{ & ig\sum_\ell A_\ell - \tfrac{1}{2}g^2 \sum_{\ell_1<\ell_2}[A_{\ell_1},A_{\ell_2}] - \tfrac{1}{4}ig^3 \sum_{\ell_1<\ell_2<\ell_3}[[A_{\ell_1},A_{\ell_2}],A_{\ell_3}] \\ & -\tfrac{1}{12}ig^3 \sum_{(\ell_1,\ell_2)<\ell_3}[A_{\ell_1},[A_{\ell_2},A_{\ell_3}]] - \tfrac{1}{12}ig^3 \sum_{\ell_1<\ell_2}[[A_{\ell_1},A_{\ell_2}]A_{\ell_2}] \\ & + g^4\times(\text{commutators with } 4A'_\ell\text{s}) + O(g^5)\Big\}\,. \end{aligned} \tag{B.2}$$

Here, $\sum_\ell$, etc., denote ordered sums along the path C of the Wilson loop which we take to have the four corners x_0, $x_0+R\hat{\mu}$, $x_0+R\hat{\mu}+T\hat{\nu}$, $x_0+T\hat{\nu}$. $\ell_1<\ell_2$ means that the link ℓ_1 comes before the link ℓ_2, and A_ℓ is

$$\begin{aligned} A_\ell &= A_\mu(x) \qquad \text{for} \qquad \ell=(x,x+\hat{\mu})\,, \\ A_\ell &= -A_\mu(x-\hat{\mu}) \qquad \text{for} \qquad \ell=(x,x-\hat{\mu})\,. \end{aligned} \tag{B.3}$$

Expanding the exponential in (B.2), taking the trace and using (i) the cyclic property of the trace, (ii) the fact that the trace of a commutator vanishes, and (iii) the fact that $A_\mu(x)$ is traceless for SU(N), we obtain the expansion coefficients of eq. (3.2):

$$\omega_2=\frac{1}{2N}\operatorname{tr}\Big(\sum_\ell A_\ell\Big)^2=\frac{1}{4N}\Big(\sum_\ell A^a_\ell\Big)^2\,,$$

$$\omega_3=\frac{i}{6N}\operatorname{tr}\Big(\sum_\ell A_\ell\Big)^3+\frac{i}{2N}\operatorname{tr}\Big(\sum_\ell A_\ell \sum_{\ell_1<\ell_2}[A_{\ell_1},A_{\ell_2}]\Big)\,,$$

$$\omega_4 = -\frac{1}{4N}\,\mathrm{tr}\left(\left(\sum_\ell A_\ell\right)^2 \sum_{\ell_1<\ell_2}[A_{\ell_1}, A_{\ell_2}]\right)$$
$$-\frac{1}{8N}\,\mathrm{tr}\left(\sum_{\ell_1<\ell_2}[A_{\ell_1}, A_{\ell_2}]\right)^2$$
$$-\frac{1}{4N}\,\mathrm{tr}\left(\sum_\ell A_\ell \sum_{\ell_1<\ell_2<\ell_3}[[A_{\ell_1}, A_{\ell_2}], A_{\ell_3}]\right)$$
$$-\frac{1}{12N}\,\mathrm{tr}\left(\sum_\ell A_\ell \sum_{(\ell_1,\ell_2)<\ell_3}[A_{\ell_1}, [A_{\ell_2}, A_{\ell_3}]]\right)$$
$$-\frac{1}{12N}\,\mathrm{tr}\left(\sum_\ell A_\ell \sum_{\ell_1<\ell_2}[[A_{\ell_1}, A_{\ell_2}]A_{\ell_2}]\right)$$
$$\bar{\omega}_4 = -\frac{1}{24N}\,\mathrm{tr}\left(\sum_\ell A_\ell\right)^4. \tag{B.4}$$

It turns out that the first terms in ω_3 and ω_4 do not contribute to the expectation value at order g^4 due to symmetry properties in the colour indices.

Appendix C

THE VACUUM POLARIZATION TENSOR

In this appendix we give the vacuum polarization tensor $\Pi_{\mu\nu}$ to order g^2 for an asymmetric $L^{d-1}\times L_d$ lattice. We split it into two parts

$$\Pi_{\mu\nu}(p) = \Pi^{(a)}_{\mu\nu}(p) + \Pi^{(b)}_{\mu\nu}(p)\,. \tag{C.1}$$

The second part comes from the four-gluon vertex $\bar{S}_2$ (see fig. 2a), and is given by

$$\Pi^{(b)}_{\mu\mu}(p) = \frac{(2N^2-3)}{3N}\,g^2\left[2I\sum_{\rho\neq\mu,d} s^2_\rho(\tfrac{1}{2}p) + (I+I_d)s^2_d(\tfrac{1}{2}p)\right] \quad \text{for } \mu\neq d,$$
$$\Pi^{(b)}_{\mu\nu}(p) = -\frac{2(2N^2-3)}{3N}\,g^2 I s_\mu(\tfrac{1}{2}p)s_\nu(\tfrac{1}{2}p) \quad \text{for } \mu\neq\nu;\ \mu,\ \nu\neq d,$$
$$\Pi^{(b)}_{dd}(p) = \frac{(2N^2-3)}{3N}\,g^2(I+I_d)\sum_{\rho\neq d} s^2_\rho(\tfrac{1}{2}p)\,,$$
$$\Pi^{(b)}_{\mu d}(p) = -\frac{(2N^2-3)}{3N}\,(I+I_d)s_\mu(\tfrac{1}{2}p)s_d(\tfrac{1}{2}p) \quad \text{for } \mu\neq d. \tag{C.2}$$

For writing convenience, we split $\Pi^{(a)}_{\mu\nu}(p)$ again into two parts:

$$\Pi^{(a)}_{\mu\nu}(p) = \Pi^{(a_1)}_{\mu\nu}(p) + \Pi^{(a_2)}_{\mu\nu}(p)\,. \tag{C.3}$$

$\Pi_{\mu\nu}^{(a_1)}$ comes from the three-gluon vertex S_1 and the last contribution from S_{FP} in (2.9). It is depicted in fig. 2b and is given by

$$\begin{aligned}\Pi_{\mu\nu}^{(a_1)}(p) = 2Ng^2 \int_k \frac{1}{D(k)D(p+k)} \Big\{ & 2\delta_{\mu\nu} c_\nu^2(\tfrac{1}{2}k) \sum_\rho s_\rho^2(\tfrac{1}{2}(2p+k)) \\ & + s_\mu(\tfrac{1}{2}(2k+p)) s_\nu(\tfrac{1}{2}(2k+p)) \Big[\sum_\rho c_\rho^2(\tfrac{1}{2}p) - c_\mu^2(\tfrac{1}{2}p) - c_\nu^2(\tfrac{1}{2}p) \Big] \\ & + 2 s_\mu(\tfrac{1}{2}(2p+k)) s_\nu(\tfrac{1}{2}(k-p)) c_\mu(\tfrac{1}{2}(p+k)) c_\nu(\tfrac{1}{2}k) \\ & - 2 s_\mu(\tfrac{1}{2}(p+k)) s_\nu(\tfrac{1}{2}k) c_\mu(\tfrac{1}{2}k) c_\nu(\tfrac{1}{2}(p+k)) \Big\} . \end{aligned} \tag{C.4}$$

$\Pi_{\mu\nu}^{(a_2)}$ comes from the four-gluon vertex S_2, the rest of S_{FP} and the measure contribution S_{meas}. It is shown in fig. 2c, and amounts to

$$\begin{aligned}\Pi_{\mu\nu}^{(a_2)}(p) = {} & \tfrac{1}{6} Ng^2 \delta_{\mu\nu} \Big\{ -I - \tfrac{1}{2} + (3d-1)\Delta_0 - (2d-4)\Delta_1 + 3\Delta_1 c_\mu(p) \\ & - (2\Delta_0 + 5\Delta_1) \sum_{\rho \neq d} c_\rho(p) - (2\Delta_0 + 4\Delta_1 + \Delta_1^d) c_d(p) \Big\} \\ & - \tfrac{2}{3} Ng^2 (\Delta_0 + \Delta_1) s_\mu(\tfrac{1}{2}p) s_\nu(\tfrac{1}{2}p) \quad \text{for } \mu, \nu \neq d , \\ \Pi_{\mu d}^{(a_2)}(p) = {} & -\tfrac{1}{3} Ng^2 (2\Delta_0 + \Delta_1 + \Delta_1^d) s_\mu(\tfrac{1}{2}p) s_d(\tfrac{1}{2}p) \quad \text{for } \mu \neq d , \\ \Pi_{dd}^{(a_2)}(p) = {} & \tfrac{1}{6} Ng^3 \Big\{ -I_d - \tfrac{1}{2} + (3d-1)\Delta_0 - (2d-4)\Delta_1^d \\ & - (2\Delta_0 + 4\Delta_1^d + \Delta_1) \sum_{\rho \neq d} c_\rho(p) - 2(\Delta_0 + \Delta_1^d) c_d(p) \Big\} \\ & - \tfrac{2}{3} Ng^2 (\Delta_0 + \Delta_1^d) s_d^2(\tfrac{1}{2}p) . \end{aligned} \tag{C.5}$$

One easily checks that the vacuum polarization tensor $\Pi_{\mu\nu}(p)$ satisfies the Bose symmetry:

$$\Pi_{\nu\mu}(-p) = \Pi_{\mu\nu}(p) , \tag{C.6}$$

and is even in the external momentum p:

$$\Pi_{\mu\nu}(-p) = \Pi_{\mu\nu}(p) , \tag{C.7}$$

The definitions of I, I_d, Δ_0, Δ_1 and Δ_1^d can be found in sect. 2.

References

[1] K.G. Wilson, Phys. Rev. D10 (1974) 2445
[2] M. Creutz, L. Jacobs and C. Rebbi, Phys. Reports 95 (1983) 201;
C. Rebbi, Lattice gauge theories and Monte Carlo simulations (World Scientific, 1983)
[3] V.F. Müller and W. Rühl, Ann. of Phys. 133 (1981) 240

[4] T. Hattori and H. Kawai, Phys. Lett. 105B (1981) 43
[5] R. Kirschner, J. Kripfganz, J. Ranft and A. Schiller, Nucl. Phys. B210 [FS6] (1982) 567
[6] G. Curci, G. Paffuti and R. Trippicione, Nucl. Phys. B240 [FS12] (1984) 91
[7] J. Engels, F. Karsch, I. Montvay and H. Satz, Nucl. Phys. B205 [FS5] (1982) 545
[8] R.V. Gavai, F. Karsch and H. Satz, Nucl. Phys. B220 [FS8] (1983) 223
[9] A. Hasenfratz, P. Hasenfratz, U. Heller and F. Karsch, Phys. Lett. 140B (1984) 76
[10] A. Hasenfratz, P. Hasenfratz, U. Heller and F. Karsch, Phys. Lett. 143B (1984) 1983
[11] B.E. Baaquie, Phys. Rev. D16 (1977) 2613;
A. Hasenfratz and P. Hasenfratz, Phys. Lett. 93B (1980) 165;
A. Di Giacomo and G. Paffuti, Nucl. Phys. B205 [FS5] (1982) 313
[12] P. Hasenfratz, Phys. Lett. 141B (1984) 385
[13] H.D. Politzer, Nucl. Phys. B236 (1984) 1
[14] A.M. Polyakov, Phys. Lett. 72B (1978) 477;
L. Susskind, Phys. Rev. D20 (1979) 2610
[15] M. Creutz, Phys. Rev. D23 (1981) 1815
[16] J.E. Hirsch and S.H. Shenker, Phys. Rev. B27 (1983) 1736
[17] A. Hasenfratz, P. Hasenfratz, U. Heller and F. Karsch, CERN preprint TH.3842 (1984), Z. Phys. C, to be published;
D. Barkai, K.J.M. Moriarty and C. Rebbi, Phys. Rev. D30 (1984) 1293
[18] A. Billoire, Phys. Lett. 104B (1981) 472;
E. Kovacs, Phys. Rev. D25 (1982) 871
[19] F. Karsch, Nucl. Phys. B205 [FS5] (1982) 285
[20] J. Engels, F. Karsch and H. Satz, Nucl. Phys. B205 [FS5] (1982) 239
[21] T. Celik, J. Engels and H. Satz, Phys. Lett. 129B (1983) 323
[22] C.P. Korthals-Altes, Cargèse Lectures, September 1983; private communications